Diamond & Related Materials 26 (2012) 25–31

Contents lists available at SciVerse ScienceDirect

Diamond & Related Materials

journal homepage: www.elsevier.com/locate/diamond

Surface integrity of PCD composites generated by dynamic friction polishing: Effect of processing conditions ☆

Y. Chen, L.C. Zhang *, F. Tang

School of Mechanical and Manufacturing Engineering, The University of New South Wales, NSW 2052, Australia

ARTICLE INFO

Available online 13 April 2012

Keywords:
Polycrystalline diamond
Composites
Dynamic friction polishing
Surface integrity
Material removal rate
Raman spectroscopy

ABSTRACT

This paper investigates the surface integrity of polycrystalline diamond composites (PCDCs) generated by an efficient abrasive-free dynamic friction polishing. The analysis includes the polishing efficiency, surface roughness, surface damage and residual stress distribution in relation to polishing conditions and microstructures on two types of thermally stable PCDCs. Raman spectroscopy revealed that transformed phases were mainly around grain boundaries, that the magnitudes of residual stresses in polished PCDCs varied across its polished surface, and that stress concentrations over 1 GPa appeared in the vicinity of grain boundaries. It was found that the PCDCs with high percentages of diamond could be polished without cracking at a much large material removal rate of 0.13 mg/s (0.037 mm^{-3}/s) under a high sliding speed and pressure combination of 35 m/s and 5 MPa, while the PCDCs with low contents of diamond were susceptible to cracking. The underlying mechanisms of sample cracking were discussed.

1. Introduction

Since the successful synthesis of diamond, especially the rapid development of chemical vapour deposition (CVD) diamond technology, various techniques using mechanical, chemical and thermal methods or a synergistic combination of them have been developed to polish the diamond surfaces [1–4]. Each polishing technique has its technological merits but also suffers from one or more disadvantages. Dynamic friction polishing (DFP) [5–10] is a newly proposed method in recent years and appears as an attractive alternative to provide the efficiency that the conventional methods cannot achieve. This abrasive-free DFP technique utilizes the thermo-chemical reaction induced by the frictional heating at the sliding interface between a diamond specimen and a rotating catalytic metal disk. The polishing time has been reduced 10 folds from 4 h to 18 min, compared to the abrasive polishing method currently used in industry [11].

In the previous studies, we have characterized both the upper and lower boundaries of temperature rise at the polishing interface [10,12], explored the material removal mechanisms [8,9], and established the polishing efficiency and polishing map [7,11] for damage free polishing. These studies were conducted on the thermally stable polycrystalline diamond composites (PCDCs) made of 65–75% diamond powder with silicon or SiC as the electrically conductive binder. However, the characterization of surface integrity of polished surfaces has not been fully investigated. The surface quality of a polished component is important because it will greatly influence the performance of the PCDC in applications [1,13,14]. A high quality surface possesses a great integrity with a much smaller friction coefficient, higher thermal resistance, lower scattering of incident light and greater electronic behavior, and enables precision applications in cutting tools, heat sinks, semiconductors and optical windows. On the other hand, a low quality surface, for instance, will cause chip build-up when using as cutting tool and reduce the tool life.

Recently, a new type of thermally stable PCDCs has been developed with a very high percentage of diamond (≥95%) and small amount of silicon. It was demonstrated that such new PCDCs have better properties, such as greater toughness and higher hardness compared to composites with lower diamond content (from unpublished experimental data). However these PCDCs cannot be processed by electrical discharge machining (EDM) due to their dielectric nature, and they are also harder to be polished by a traditional method compared with the normal Si/SiC-bonded PCDCs. The applications of this type of superior materials have been restricted, and they have been mainly used as-sintered for rough operations, such as for drilling tools in oil and geological industries that do not need precision.

Raman spectroscopy is one of the principal characterization methods for Si and diamond materials, and has been utilized to investigate the phase transformation and residual stress distribution [15–20]. It is able to distinguish different forms of Si and carbon, including crystalline materials and various possible non-crystalline phases. In addition, the method of stress-induced linear shift in peak positions can be used to estimate stresses in diamond films and Si materials [16,17,20,21].

☆ Presented at the Diamond 2011, 22st European Conference on Diamond, Diamond-Like Materials, Carbon Nanotubes, and Nitrides, Budapest.

* Corresponding author.
E-mail address: Liangchi.Zhang@unsw.edu.au (L.C. Zhang).

0925-9635/$ – see front matter © 2012 Elsevier B.V. All rights reserved.
doi:10.1016/j.diamond.2012.04.002

Aiming to improve the surface integrity of the polished PCDCs and explore the possibility of fast polishing of this new type of PCDCs using the abrasive-free DFP method to extend their applications, this paper investigates the material removal rates and characterization of surface integrity, including the surface roughness, surface damage and residual stress distribution with the aid of surface analyser, electron microscopy and Raman spectroscopy.

2. Experiments

Two types of thermally stable PCDCs were used for the experiment, as shown in Table 1. The Type 1 PCDCs contains over 95 wt.% of poly-crystalline diamond particles in a wide range of grain sizes with an initial surface roughness of Ra ≈ 4 μm. The Type 2 PCDCs has about 70–75% diamond particles of ~25 μm in grain size (the rest are SiC and Si) with an initial surface roughness of Ra ≈ 1.7 μm. A typical specimen used in experiment was 12.7 mm in diameter and 4 mm in thickness, weighing approximately 1.7 g.

The dynamic friction polishing experiments were carried out on a polishing machine manufactured in-house [22]. Polishing, as detailed in [11], was conducted by pressing a rotating PCDC specimen at a predetermined pressure on to a rotating stainless steel disk in a dry atmosphere. The sliding speed between the specimen and the metal disk varied from 10 to 35 m/s. The applied polishing pressures were 1.0, 2.2, 2.7, 3.1, 3.8 and 5.0 MPa. After polishing, the surface was cleaned with acid solution and/or by mechanical rubbing on an Al_2O_3 sand paper before weight-loss measurement and Raman analysis. The effect of this mechanical cleaning on surface roughness is negligible as the PCDCs are much harder than the Al_2O_3.

The surface roughness values were measured using Surftest 402 and Surftest Analyzer (Mitutoyo). The surface morphology of the specimens, including micro-cracks, was examined using an optical microscope (Leica DM RXE) and a field emission scanning electron microscope (SEM, FEI Nova NanoLab). The SEM examination was carried out at 20 kV with a 5 mm working distance. The amount of removed materials was determined by measuring the weight loss and thickness change of a PCDC specimen before and after polishing, and the data based on the two means are comparable. The specimen weight was measured on an electronic balance (Sartorius Basic plus BP210D, resolution of 0.01 mg). The thickness of a specimen was measured by a micrometer, a comparator and slip gauges. The readability of the comparator was 2.5 μm.

Raman spectra were collected using a Renishaw Raman InVia Reflex equipped with a charge-coupled device (CCD) camera, where the collection optics was based on a Leica DMLM microscope. The zones for the recording of spectra were selected optically, and they were excited by an argon 514.5 nm laser. Spectra were obtained by using a microscope objective lens (×50) to focus the incident power (at 10 mW) onto the PCDC surface with a spot size of about 1.5 μm. Daily calibration of the wave-number axis was achieved by recording the Raman spectrum of silicon (one accumulation, 10 s) for both static and extended modes. Raman maps were generated by collecting the spectra from selected areas from a PCDC sample with the step size of 1 μm. The spectral acquisition parameters were as follows: extended mode, grating position from 200 to 1700 cm^{-1}, 1 scan, 10 s exposure, ×50 objective. A representative spectrum from the map dataset was curve fitted using the initial parameter Gaussian–Lorentzian mixture and the resultant curve-fitting parameters were saved. A map of the band position was then produced by fitting the individual spectra within the map dataset using the previously saved parameters.

Table 1
Specifications of the PCDCs used in experiment.

	Type 1	Type 2
Diamond percentage (wt.%)	>95	70–75
Grain size of the polycrystalline diamond (μm)	Varied	~25
Surface roughness Ra (μm)	4	1.7
Size: Diameter (mm) × thickness (mm)	12.7 × 4	12.7 × 4

3. Results and discussion

3.1. Material removal rate

Fig. 1 shows the variations of the material removal rates at different sliding speeds and pressures for both types of the PCDCs at a given polishing time. The symbols represent the experimental results, while the solid lines are the fitted linear regression lines. Fig. 1(a) is for Type 1 PCDCs specimens having an initial Ra ~4 μm at a fixed polishing duration of 6 min, and Fig. 1(b) is for Type 2 PCDCs specimens with an initial Ra ~1.7 μm at a fixed polishing time of 3 min.

It can be seen that for both types of the PCDCs, the polishing rates are the functions of pressure and sliding speed, and are on the same order when being polished under the same nominal conditions. At a given sliding speed, the material removal rate increases with the rising of pressure. Similarly, a higher speed at a given pressure results in a higher removal rate. However, cracking occurred in Type 2 PCDCs at the high speed–pressure combinations [11], i.e., above the dotted line in Fig. 1(b) under the following polishing conditions, e.g., pressure = 5 MPa and sliding speed ≥ 16 m/s; pressure = 3.8 MPa and sliding speed ≥ 20 m/s; and pressure = 3.1 MPa and sliding

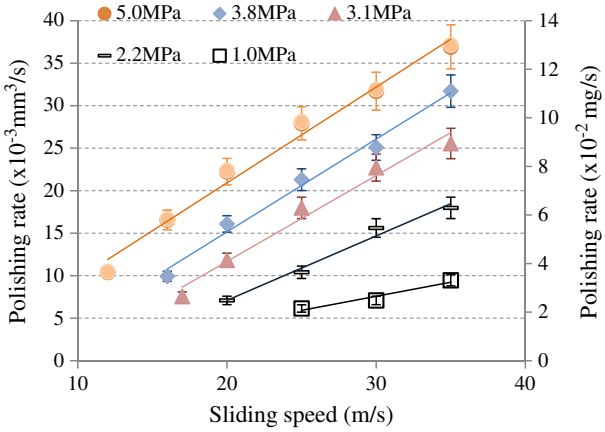

(a) Type 1 PCDC

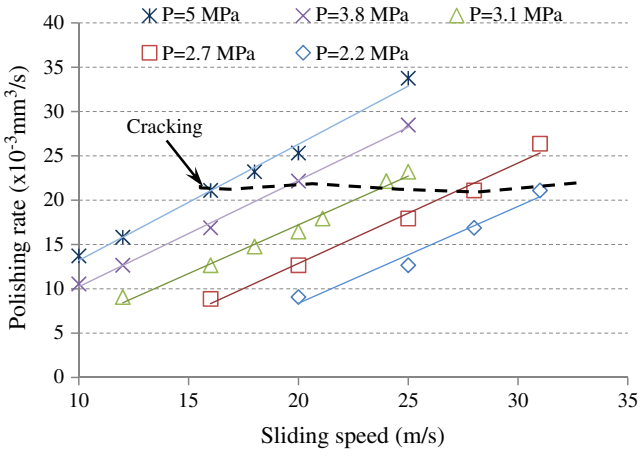

(b) Type 2 PCDC (derived from [11])

Fig. 1. Variations of polishing rates with different sliding speeds and pressures.

speed ≥ 24 m/s. Furthermore, it was found that the cracking gets more significant with the polishing time under the same sliding speed and pressure [11]. The highest material removal rate without cracking is approximately 0.021 mm^{-3}/s. Only with some range of pressure–speed combination, could a damage-free polishing with a reasonable material removal rate be obtained.

On the contrary, no cracking was found on the Type 1 PCDCs under all of the above polishing conditions with even a much increased speed of 35 m/s, pressure of 5 MPa and polishing time of 6 min. Though the Type 1 PCDCs cannot be processed by EDM and are much more difficult to be polished by a conventional method compared to Type 2 PCDC, they could be polished to achieve cracking-free surfaces at a high material removal rate under higher pressure–speed combinations. For example, a very high polishing rate of 0.13 mg/s (0.037 mm^{-3}/s) can be achieved at the sliding speed of 35 m/s and pressure of 5 MPa.

3.2. Surface topography

Fig. 2 shows the SEM images of a typical PCDC specimen before and after polishing, where panels (a) and (b) are from Type 1 PCDCs and panels (c) and (d) from Type 2 PCDCs. It should be noted that the surface of specimen was tilted to 52° inside the SEM chamber in order to improve the observation of surface morphology.

Prior to polishing, Fig. 2(a) shows the as-sintered rough Type 1 PCDC surface with a roughness value of Ra ≈ 4 μm. It illustrates some features of crystals such as relative 'plate' surfaces and sharp edges. Individual diamond grains are not directly visible because some crystals chipped off and their surfaces, edges and corners could no longer be distinguished. On the other hand in Fig. 2(c), Type 2 PCDCs had better surface finish (Ra ≈ 1.7 μm) before polishing since they were shaped by electrical discharge machining (EDM) to the required dimensions. It demonstrates a surface with 'granular' particles almost without any crystalline features. This remarkable difference of surface morphology may be closely related to the EDM process.

After polishing, the surface roughness of both Types of PCDCs was sharply reduced to 0.1 to 0.5 μm Ra depending on the applied polishing conditions. For instance, a surface roughness of ~0.3 μm Ra was measured in the specimen shown in Fig. 2(b) which was polished for 6 min at 30 m/s sliding speed with a pressure of 5 MPa. On the other hand, though the Type 2 PCDCs had a better initial surface finish, it ended up with a similar level of surface finish (without cracking) as that of Type 1 PCDC after the polishing at the sliding speed of 20 m/s with a pressure of 3.1 MPa.

In Fig. 2(b) and (d) of the polished specimens, although a slightly uneven surface is discernible among diamond grains, it obviously presents a smoother surface across the entire PCDC compared to that without polishing. Another striking feature in the polished surface was the various wear tracks, such as the array of 'grooves', which is studied in another paper [23].

For Type 1 specimen, Fig. 2(b) also presents a wide distribution of grain sizes ranging from a few microns to up to a hundred microns. This is in line with the fabrication of PCDCs where diamond particles

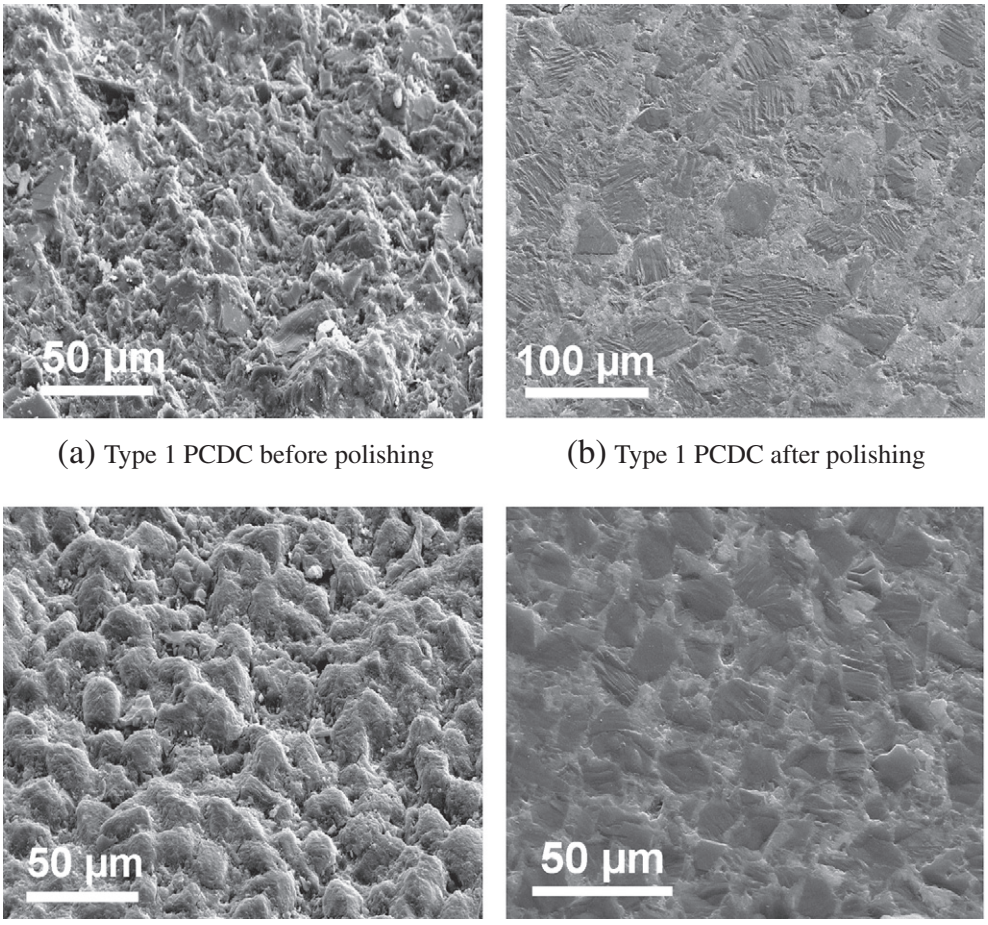

(a) Type 1 PCDC before polishing (b) Type 1 PCDC after polishing

(c) Type 2 PCDC before polishing (d) Type 2 PCDC after polishing

Fig. 2. SEM images of the Type 1 PCDC surfaces.

with various grain sizes were employed, although the pulverization of large diamond particles during the PCDCs manufacturing process [24] might also act as another contributor.

On the contrary, the polished PCDC surface of Type 2 depicts a fairly uniform grain size (~20–30 μm) in Fig. 2(d), although with inclusion of some fine grains. It is clear that the microstructure of sintered PCDCs in which diamond grains with somewhat crystalline shapes are embedded in an almost continuous binder phase is readily indentified in these polished specimens.

The resulting high quality surface finish for both types of PCDCs unanimously demonstrates a significant advantage of DFP polishing which has a capability of processing a PCDC with an extremely high content of diamond grains (>95%).

3.3. Phase transformation and residual stress distribution

It is known that amorphous, cubic and hexagonal forms of Si and carbon can be differentiated based upon their Raman spectra [18,19]. Furthermore, Raman peaks shifted from their stress free position, e.g., diamond peaks at 1332 cm^{-1} and Si peak at 520 cm^{-1}, provide information on residual stresses. It has been reported that the Raman peak position tends to shift linearly to lower wavenumbers under tensile strains and to higher wavenumbers under compressive strains [20]. Since it was difficult to identify the orientation of Si or diamond crystals in a PCDC, the residual stress was evaluated by averaging the stress shift relation over all crystallite orientations. The magnitude of stress within the PCDC Raman shift is known proportional to the Raman shift, and the stress for diamond can be estimated as [15,24,25]:

$$\sigma = -0.567(\omega_m - \omega_0)(\text{GPa}) \quad (1)$$

where $\omega_0 = 1332\ cm^{-1}$ is the stress-free diamond peak, and ω_m is the measured Raman peak position. If the Raman shift splits into two, ω_m is the medium position between the two components ω_1 and ω_2,

$$\omega_m = 0.5(\omega_1 + \omega_2). \quad (2)$$

Similarly, the stress for the Si can be estimated as [20,26]

$$\sigma = -0.27\left(\omega_m - \omega_{0,Si}\right)(\text{GPa}) \quad (3)$$

where $\omega_{0,si} = 520\ cm^{-1}$ is the stress-free Si peak (as the daily calibrated Si reference peak position). In these equations, $\sigma<0$ and $\sigma>0$ correspond to the compressive and tensile stress, respectively.

3.3.1. Type 1 PCDCs

The Raman spectra obtained on a PCDC surface before polishing are shown in Fig. 3. The Raman peak at 1332 cm^{-1} predominates most of the collected spectra, indicating a stress-free diamond composite. Since this type of PCDCs contains more than 95% of diamond, the Raman peak of other material elements can hardly be detected at any spot of the surface, except rarely some low intensity graphite bands at ~1585 cm^{-1} are observable.

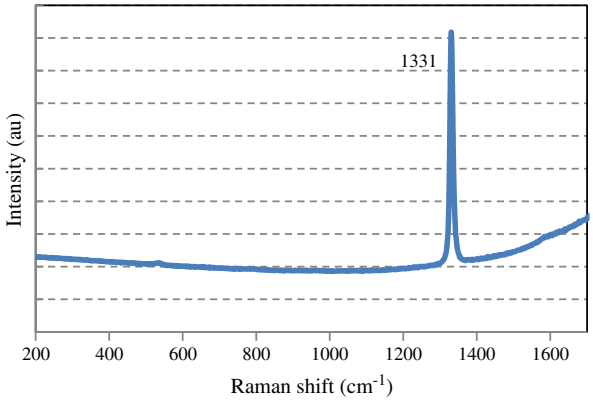

Fig. 3. Raman spectra of Type 1PCDC specimens before polishing.

After polishing at the sliding speed of 35 m/s and pressure of 3.8 MPa for 6 min, a surface roughness of 0.3 μm Ra could be reached without surface micro-cracks. The results of Raman analysis on a polished surface is shown in Fig. 4. Fig. 4(a) shows an optical image of the polished surface, and the marked area for Raman stress mapping and labeled spots for typical Raman spectra. Fig. 4(b) demonstrates the stress distribution as a function of diamond peak position calculated from Eq. (1) in the area marked in Fig. 4(a). Though the stress on the surface appears to be non-uniform across the examined entire area, it is evenly distributed within the diamond grain, very low close to zero.

The typical Raman spectra from positions of 'A' to 'D' in Fig. 4(a) are given in Fig. 4(c), and their stress values calculated from diamond Raman shifty by Eq. (1) are shown in Table 2. In most areas the examined dominated Raman peaks are attributed to the diamond. The transformed non-diamond carbon phases only occasionally appeared in some grain boundaries. High intensity of Raman peak A at around 1332 cm^{-1} which is the fingerprint of the diamond is predominant over the diamond grain area. This indicates that the low stress at almost zero is evenly distributed over the whole diamond grain. Between the large diamond grain and the right next smaller one, there are no other non-diamond peaks detected. However, on the dark spot of the smaller grain, though the diamond peak B is still very strong, the peak position shifts to1330 cm^{-1}, representing a tensile stress of ~1.130 GPa, as shown in Fig. 4(b). Raman spectrum C is detected on the position of boundary between small grains in Fig. 4(a). In addition to the stress-free diamond peak at slightly less intensity, a broad band of amorphous carbon at 1590 cm^{-1} is also observed. On another boundary between the largest and a tiny grain, the Raman spectrum D has lower intensity. It can been seen that the peak position of diamond shifts slightly from 1332 cm^{-1} to 1331 cm^{-1} which shows a residual stress around 0.57 GPa. There are also a broad band of amorphous carbon at 1588 cm^{-1} and weak disordered SiC bands centered at 793 and 966 cm^{-1}. These results suggest that the lower percentage of SiC is scatteredly distributed in grain boundaries, and that diamond had transformed into amorphous non-diamond carbon. As polishing continues, most of transformed softer carbon materials had been removed, leaving a very small amount of such phases trapped in the grain boundaries.

3.3.2. Type 2 PCDCs

The Raman spectra of Type 2 PCDC before polishing are given in Fig. 5. Since the unpolished surface was too rough to focus under optical microscope, the correlation of spectrum and the examined position was not able to be resolved. However, the different intensities of diamond, SiC or Si band detected across different places indicate an uneven distribution of these materials. According to Fig. 5, the sharp intense band at 1332 cm^{-1} represents stress free diamond, while the peaks at 519 and 520 cm^{-1} stand for low tensile or free stress

Table 2
Stress calculation at different regions in a Type 1 PCDC.

Region	Diamond ω_m (cm^{-1})	Diamond σ (GPa)
A: Over diamond grain area	1332	0
B: The dark spot of the smaller diamond grain	1330	−1.13
C: Small grain boundary	1332	0
D: Boundary between the largest and tiny grain	1332	0.57

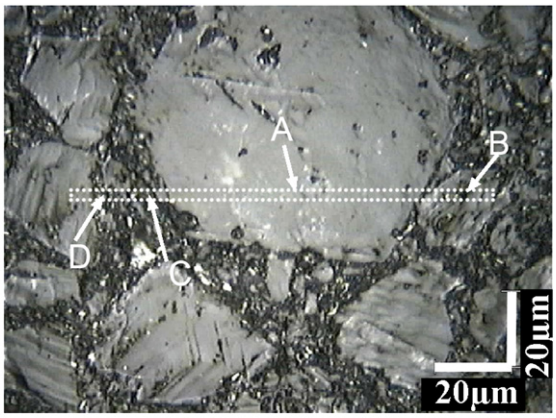

(a) Polished surface and marked for stress map area and spots for typical Raman spectra

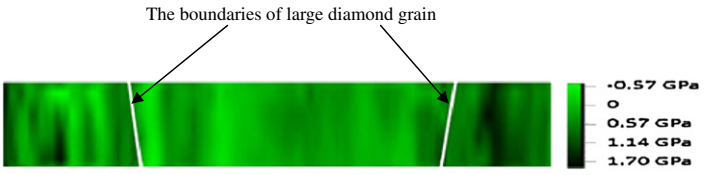

(b) Stress distribution in the marked area in (a)

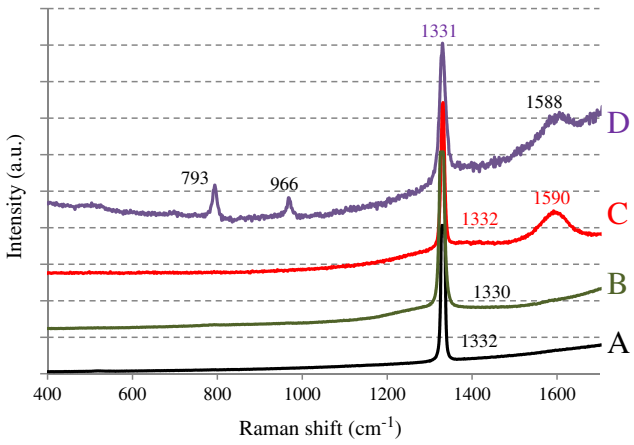

(c) Typical Raman spectra collected from the positions marked in (a)

Fig. 4. Raman spectra and stress distribution in a polished Type 1 PCDC.

of Si, and the weak band at 796 cm^{-1} is attributed to heavily disordered SiC [9].

After polishing at the sliding speed of 25 m/s and pressure of 3.1 MPa for 3 min, the surface roughness was reduced to 0.3 μm Ra, but micro-cracks appeared on the surface. Typical micro-Raman spectra at different positions of the PCDC surface (Fig. 6(a)) are shown in Fig. 6(b). It can be seen that different regions have different Raman shifts, hence different levels of residual stresses. Table 3 lists the stress values for the spectra calculated by Eqs. (1)–(3) from diamond and Si Raman shift.

The spectrum A shown in Fig. 6(b) collected from the diamond grain noted as region A, contains a high intensity of diamond peak at ~1332 cm^{-1} and a weak silicon peak at ~524 cm^{-1}, indicating stress free diamond and compressive stress state of silicon of ~1.08 GPa.

Spectrum B in Fig. 6(b) is detected from near the diamond crystal edge. The Raman peak of diamond at this region B shifts from 1332 cm^{-1} to 1329 or 1330 cm^{-1}, while Si peak shifts to 528–531 cm^{-1}. Some silicon peaks split, which can be fitted by the sum of two Lorentzian–Gaussian components peak that at 522 and 535 cm^{-1}. The magnitude of the stress is estimated to be 1.701 GPa (tensile) for diamond and 2.16–2.87 GPa (compressive) for Si at the crystal edge.

A number of Raman peaks were detected in spectrum C collected from the crack or grain boundaries: a very high intensity of Si peak at ~522 cm^{-1}, a deformed/amorphous SiC band centered at ~794 cm^{-1}, a weak amorphous carbon band at ~1584 cm^{-1} and a very low intensity of diamond peak at ~1332 cm^{-1}. Since the evaluated stresses were low for both diamond (almost zero) and silicon (at ~0.54 GPa compressive), it is rational that the cracking had an effect in the releasing of stresses around this region. This result also indicates that the crack could occur in the vicinity that contains Si/SiC components and around the grain boundaries of diamond.

In some large crack areas (e.g., spot D), in addition to the Si peak at 526 cm^{-1} and amorphous carbon band at 1590 cm^{-1}, the spectrum

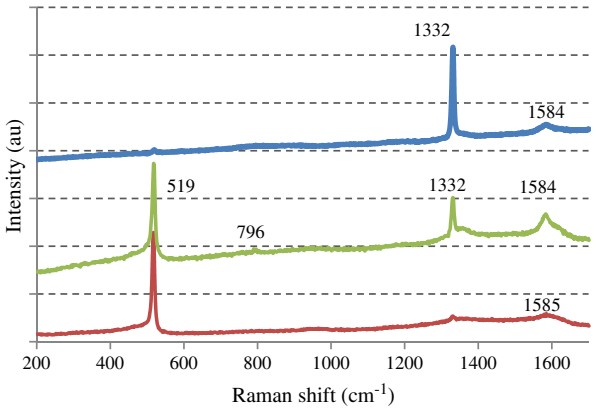

Fig. 5. Typical Raman spectra of Type 2PCDC specimens before polishing.

also contains a diamond peak of 1332 cm^{-1} with a reduced intensity, which was likely collected from the diamond grains underneath the surface.

Though there is uncertainty regarding orientation of the crystals and direction of strain, the calculated magnitudes of stress may differ from the actual values; Raman analysis can directly provide important information on the local stress variations in the sample, and give a first indication on the sign and distribution of the stress.

From the above analysis, it can be seen that stresses in PCDCs are not uniformly distributed but rather localized near crystal edges. The stress level in Type 2 PCDCs is higher than that of Type 1 PCDCs. The higher values are often observed between adjoining crystals, which leads to the cracking along the diamond grains.

3.4. Surface finish and underlying mechanism of cracking

From Section 3.1, it is noted that cracking occurred on Type 2 PCDCs at the high speed–pressure combinations [11]. On the contrary, Type 1 PCDCs could be polished to achieve cracking-free surfaces at a high material removal rate under higher pressure–speed combinations, as no cracking was found on the Type 1 PCDCs under all of the above polishing conditions.

In addition to the mechanical stresses under a polishing pressure, non-uniform thermal stresses could contribute to the cracking due to the mismatch of the thermal expansion coefficients of diamond and silicon. This becomes particularly significant in Type 2 PCDCs. For instance, in Raman analysis of cracked area, Si and SiC are the main phases, with little amorphous graphite and very weak diamond. In the grain areas, however, diamond is dominant. This observation indicates that cracking occurred along the diamond and SiC boundaries. When the polishing temperature increases under a high speed–pressure combination, the thermal stresses increase to a high level to cause cracking along the PCD–SiC boundaries. The thermal stress can be estimated by [16,25],

$$\sigma = \frac{E}{1-\upsilon}\int_{20^{\circ}C}^{T}(\alpha_d - \alpha)dT, \tag{4}$$

where E is Young's modulus, α_d and α are the thermal-expansion coefficients of diamond and silicon/SiC, ν is the Poisson ratio, and T is the polishing temperature.

For the Type 2 specimen, E is 860 GPa [27], and Poisson ratio is 0.09. The thermal-expansion coefficients are 1×10^{-6}/K for diamond, 3.0×10^{-6}/K for Si and 2.8×10^{-6}/K for SiC at 300 K. The coefficients for the three materials increase with temperature, but the disparity between the coefficients decreases as temperature increases, and they all have similar value of ~4.3×10^{-6}/K at 1000 K [28]. During polishing, the approximate interface temperatures need to be over 1000 K for workable material removal [10,12], and therefore all components (diamond, Si and SiC) have similar thermal expansion coefficient. When the temperature decreases rapidly after polishing, because the coefficient of silicon/SiC is much greater than that of diamond, the bind phases of silicon/SiC contract more, therefore they experience higher compression stresses as verified by Raman stress analysis shown in Table 3 and Fig. 6(b). At the edge of diamond crystals, diamond surrounded by silicon and contracts less than silicon, thus could experience tensile stress. If these stresses are high enough when a PCDC is polishing at high speed–pressure combination, they will force apart the binder phases from diamond grains and result in cracking along the grains.

Since the Type 1 PCDCs are made of a very high percentage of diamond, the thermal stresses caused by the mismatch of thermal expansion coefficients were negligible according to Eq. (4). The stresses are smaller and distributed more evenly comparing to Type 1 PCDC, as shown in Fig. 4. Therefore no crack was developed.

From the above analysis it is clear that the DFP process has shown a promising application in polishing PCDCs even with extremely high diamond contents (>95%). A high quality surface of ~0.3 μm Ra can be accomplished under an optimum speed–pressure polishing combination with successfully avoiding cracks. Following DFP processing, an even fine surface finish at Ra ~50 nm on PCDCs has been further obtained by an additional slightly mechanical polishing for 15 min, which could further extend application of PCDCs.

4. Conclusions

The PCDCs with higher percentages of diamond, which cannot be processed by EDM and are hard to be polished by a conventional

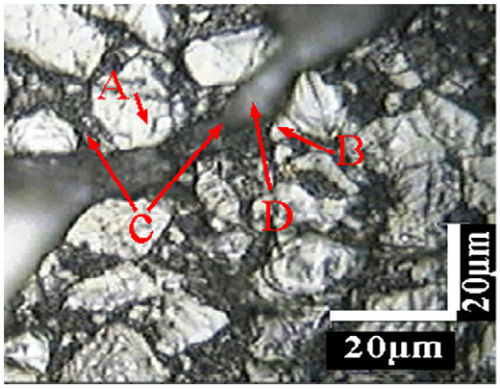

(a) Polished surface with a crack

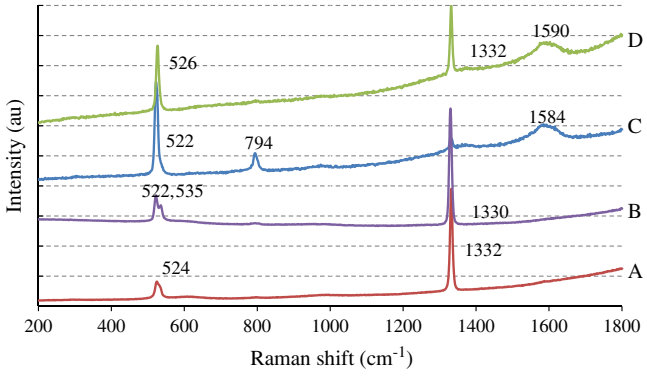

(b) Typical Raman spectra

Fig. 6. Raman spectra in a polished Type 2 PCDC surface with a crack.

Table 3
Stress calculation at different regions in a Type 2 PCDC.

Region	Diamond ω_m (cm^{-1})	Diamond σ (GPa)	Si ω_m (cm^{-1})	Si σ (GPa)
A: Middle grain	1332	0	524	1.08
B: Crystal edge	1329	−1.701	528–531	2.16–2.81
C: Crack or boundary	1332	0	522	0.54
D: Some big crack	1332	0	526	1.62

method previously, can be polished by the abrasive-free dynamic friction technique, with crack-free surfaces at a higher material removal rate. A very high polishing rate of 0.13 mg/s (0.037 mm^{-3}/s) has been obtained at the sliding speed of 35 m/s and pressure of 5 MPa, and the surface roughness has been reduced from approximately 4 μm to 0.3 μm Ra in 6 min. In addition to the mechanical stresses applied through the polishing pressure, the thermal stresses caused by the mismatch in thermal expansion coefficients of different material phases contributed to the sample cracking. Transformed phases were mainly around grain boundaries. The magnitudes of residual stresses in polished PCDCs varied across its polished surface, and stress concentrations appeared in the vicinity of grain boundaries.

Acknowledgements

The authors appreciate the Australian Research Council for their financial support to this research.

References

[1] A.P. Malshe, B.S. Park, W.D. Brown, H.A. Naseem, Diamond Relat. Mater. 8 (7) (1999) 1198.
[2] V.G. Ralchenko, S.M. Pimenov, in: M.A. Perlas, G. Popovici, L.K. Bigelow (Eds.), Handbook of Industrial Diamonds and Diamond Films, Marcel Dekker, New York, 1998, p. 983.
[3] B. Bhushan, V.V. Subramaniam, B.K. Gupta, Diamond Films Technol. 4 (2) (1994) 71.
[4] Y. Chen, L.C. Zhang, Key Eng. Mater. 407–408 (2009) 436.
[5] M. Iwai, Y. Takashima, K. Suzuki, T. Uematsu, 7th International Symposium on Advances in Abrasive Technology, 2004, Buras, Turkey.
[6] K. Suzuki, M. Iwai, T. Uematsu, N. Yasunaga, Key Eng. Mater. 238–239 (2003) 235.
[7] Y. Chen, T. Nguyen, L.C. Zhang, Int. J. Mach. Tools Manuf. 49 (2009) 515.
[8] Y. Chen, L.C. Zhang, J. Arsecularatne, Int. J. Mach. Tools Manuf. 47 (2007) 2282.
[9] Y. Chen, L.C. Zhang, J.A. Arsecularatne, Int. J. Mach. Tools Manuf. 47 (10) (2007) 1615.
[10] Y. Chen, L.C. Zhang, J.A. Arsecularatne, C. Montross, Int. J. Mach. Tools Manuf. 46 (6) (2006) 580.
[11] Y. Chen, L.C. Zhang, Int. J. Mach. Tools Manuf. 49 (2009) 309.
[12] Y. Chen, L.C. Zhang, J. Arsecularatne, Key Engineering Materials 381–382 (2008) 513.
[13] B. Bhushan, V.V. Subramaniam, A. Malshe, B.K. Gupta, J. Ruan, J. Appl. Phys. 74 (6) (1993) 4174.
[14] S.K. Choi, D.Y. Jung, S.Y. Kweon, S.K. Jung, Thin Solid Films 279 (1–2) (1996) 110.
[15] W. Fortunato, A.J. Chiquito, J.C. Galzerani, J.R. Moro, J. Mater. Sci. 42 (17) (2007) 7331.
[16] J.W. Ager, M.D. Drory, Phys. Rev. B 48 (4) (1993) 2601.
[17] H. Windischmann, K.J. Gray, Diamond Relat. Mater. 4 (5–6) (1995) 837.
[18] D.S. Knight, W.B. White, J. Mater. Res. 4 (2) (1988) 385.
[19] Y. Gogotsi, C. Baek, F. Kirscht, Semicond. Sci. Technol. 14 (1999) 936.
[20] E. Anastassakis, J. Appl. Phys. 86 (1) (1999) 249.
[21] M.S. Amer, L. Durgam, M.M. El-Ashry, Mater. Chem. Phys. 98 (2–3) (2006) 410.
[22] L.C. Zhang, B. Oliver, Y. Chen, and J.A. Arsecularatne, Method and apparatus for polishing diamond and diamond composites, Patent No. WO/2007/147214.
[23] F. Tang, Y. Chen, L. Zhang, Philos. Mag. (2012) 1.
[24] M. Wieligor, T.W. Zerda, Diamond Relat. Mater. 17 (1) (2008) 84.
[25] V.G. Ralchenko, A.A. Smolin, V.G. Pereverzev, E.D. Obraztsova, K.G. Korotoushenko, V.I. Konov, Y.V. Lakhotkin, E.N. Loubnin, Diamond Relat. Mater. 4 (5–6) (1995) 754.
[26] P. Lengsfeld, N.H. Nickel, J. Non-Cryst. Solids 299-302 (Part 2) (2002) 778.
[27] Y. Chen, Polishing of polycrystalline diamond composites, 2007 PhD thesis, The University of Sydney.
[28] G.A. Slack, S.F. Bartram, J. Appl. Phys. 46 (1) (1975) 89.